Geometric Accuracy and Measurement Repeatability of Mobile Laser Scanning in Urban Areas of the Czech Republic

Petr Jašek[1], Dana Kousalová[1], Eva Štefanová[2*]

[1] Geodetická kancelář Nedoma & Řezník, s.r.o., Czech Republic - jasek@nedomareznik.cz, kousalova@nedomareznik.cz
[2] Charles University, Faculty of Science, Department of applied geoinformatics and cartography, Czech Republic - eva.stefanova@natur.cuni.cz

Keywords: Mobil Laser Scanning, Geometric Accuracy, Measurement Repeatability, Environmental Influences, Point Cloud Analysis

Abstract

Mobile Laser Scanning is an effective method for collecting high-resolution spatial data. The assessment of the geometric accuracy of the point clouds remains a key topic in land surveying. This paper focuses on the evaluation of the internal geometric accuracy and measurement repeatability of data acquired by the RIEGL VMX-2HA mobile laser scanning system. The objective of the research is to assess the system's ability to generate spatially consistent outputs under identical input conditions. It is important to identify and quantify the influence of selected environmental variables such as the condition of the road surface, current meteorological conditions and time of day during data collection. The experimental part was conducted in the form of ten individual test runs along an identical route in an urban area in the city of Prague, the Czech Republic. Each test run was conducted under various scenarios – on dry and wet surfaces, at different hours of the day (morning, midday and evening hours), and under variable weather conditions. A combination of spatial statistics and point cloud comparison techniques was used to evaluate repeatability, focusing on the road surface. The results show that the RIEGL VMX-2HA mobile laser scanning system has a high level of internal accuracy under standard conditions. Specific environmental conditions may cause a slight increase in measurement uncertainty (e.g., a wet road surface). The observed deviations remain within the tolerance limits defined for standard engineering and land surveying applications.

1. Introduction

Mobile laser scanning (MLS) represents a modern technology for the rapid and highly detailed acquisition of spatial data in a wide range of environments. By integrating a laser sensor, an inertial measurement unit (IMU), and geodetic GNSS satellite systems receiver(s), it is possible to generate a point cloud with density and accuracy at the centimetre to millimetre level, at scanning rates ranging from several hundred thousand up to millions of points per second.

In addition to the accuracy of control point determination, a key parameter in evaluating the quality of MLS is the internal accuracy of the system, referred to as repeatability, which describes the consistency and stability of measurements within a single dataset, regardless of its absolute georeferencing. In other words, it indicates the extent to which similar results can be obtained when the same data acquisition and processing procedure is applied.

In current geodetic practice, various MLS are employed, ranging from SLAM scanners carried by an operator or, for example, mounted on a drone, to lidar systems primarily designed for airborne platforms. The objective of this experiment is to verify the internal accuracy of the car-mounted mobile mapping system Riegl VMX-2HA through a practical test, which includes the measurement of reference control points, subsequent data acquisition (10 datasets), and their evaluation.

2. Riegl VMX-2HA Mobile Unit

For the testing, the Riegl VMX-2HA mobile unit was used. The unit integrates a pair of Riegl VUX-1HA laser scanners, an inertial measurement unit (IMU), and a multi-frequency GNSS receiver. This configuration enables precise determination of position and orientation during motion, thereby ensuring the georeferencing of the resulting point cloud.

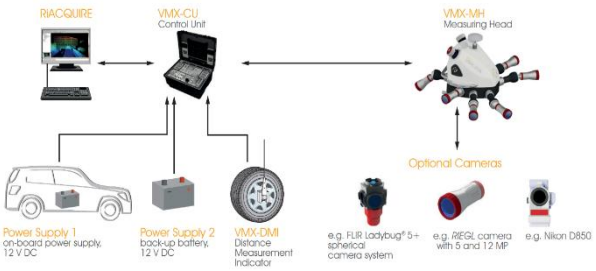

Figure 1. Riegl VMX-2HA system

Main technical parameters of the Riegl VMX-2HA:
- Number of scanners: 2 × VUX-1HA
- Maximum data acquisition rate: up to 2,000,000 points/s
- Maximum range: 420 m
- Measurement accuracy: 5 mm (standard deviation).

3. Determining Control Points

For the purpose of establishing a reference framework and the subsequent transformation of the point cloud into the S-JTSK coordinate system, control points were determined. A total of 8

* Corresponding author

control points were established and distributed to provide uniform coverage of the surveyed area.

Figure 2. Riegl VMX-2HA mounted on Škoda Yeti 2.0 TDi 81kW 4x4

All points were stabilized in the field by applying a white spray-painted checkerboard target (square side of 0.2 m), see Figure 3, and were marked to allow for inspection and repeated measurement.

Figure 3. Control point detail

The process of determining the control points was carried out in two stages:

3.1 GNSS Measurement Using the RTK Method

The control points were first determined using GNSS technology in RTK mode. These measurements provided approximate coordinates, which subsequently served as the initial adjustment. The measurements were performed twice on 23rd May 2025 (with a two-hour interval).

3.2 Measurement of the Spatial Network with a Total Station

To achieve higher accuracy, the points were surveyed using a Leica MS50 total station. The measurements were carried out from three free stations in two faces of the telescope. To increase the rigidity and stability of the spatial network, four auxiliary points were also established. The adjustment was performed in EasyNet software. A total of 66 observations were made, with 5 outliers excluded (2 × zenith angle, 3 × slope distance). After removing the outliers, 17 redundant observations remained. The final coordinates (X, Y, Z), including the achieved standard deviations (s_X, s_Y, s_Z), are presented in the following table. Points 101-104 represent the auxiliary points, while points 1001-1004 are the ground control points used for later point cloud adjustment and georeferencing. A graphical representation is provided in Figure 4.

Point ID	Y[m]	X[m]	Z[m]	s_Y [mm]	s_X [mm]	s_Z [mm]
101	734705,900	1048313,120	271,510	1,4	0,8	0,3
102	734688,402	1048303,257	271,141	1,1	0,8	0,3
103	734749,393	1048185,045	264,427	1,4	0,5	0,4
104	734732,641	1048180,086	264,295	0,9	0,9	0,4
1001	734754,729	1048107,521	259,737	2,2	1,0	0,6
1002	734743,503	1048107,302	259,740	2,1	1,0	0,6
1003	734711,722	1048245,640	268,290	1,1	0,8	0,3
1004	734722,075	1048248,043	268,233	1,2	0,6	1,0
1005	734694,209	1048341,142	272,942	1,1	1,1	0,3
1006	734681,064	1048337,929	273,071	1,4	0,6	0,3
1007	734698,228	1048429,308	276,849	2,0	1,2	0,6
1008	734706,976	1048424,180	276,743	2,0	1,2	0,6
9501	734673,289	1048361,159	275,897	0,9	0,5	0,3
9502	734717,710	1048271,166	270,851	0,8	0,6	0,2
9503	734752,531	1048170,024	265,425	0,9	0,4	0,3

Table 1. Result control points coordinates with achieved accuracies.

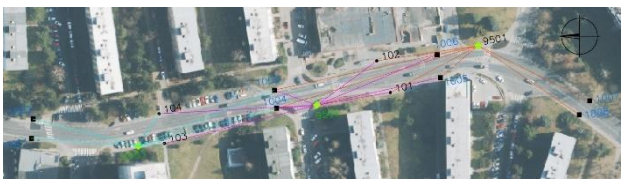

Figure 3. Observation plan

4. Data Acquisition Procedure

Data acquisition was conducted on a test section 350 meters in length (with overall recording distance 550 meters, approximately 70 meters before and after the control points) in an urban environment, featuring an elevation change of 26 meters and two curves. This setup allows the simulation of real operational conditions with varying geometry and terrain height. A total of ten passes were performed on different days and at different times of day, six under dry conditions and four under wet conditions, to account for the influence of weather on GNSS and laser scanning quality. Vehicle speed did not exceed 50 km/h, with several stops at different locations during various passes due to pedestrians and other common obstacles. Detailed weather conditions are presented in the table 2.
The test section was scanned during each of the ten passes using the Riegl VMX-2HA mobile scanning system, with data acquisition controlled directly from the vehicle via the control unit. The scanning system was operated using RiACQUIRE MLS

software, which ensures synchronized recording of laser measurements and GNSS/IMU data during motion. Prior to data acquisition, a static alignment was performed, during which the IMU is calibrated, and the system is synchronized with the reference framework.

Pass no.	Date	Time	Weather	Surface Status	Temperature °C
1	4.4.2025	14:30	Sunny	Dry	18
2	9.4.2025	7:00	Cloudy	Dry	3
3	9.4.2025	15:00	Cloudy	Dry	10
4	23.04.2025	7:00	Mostly Sunny	Dry	7
5	23.04.2025	14:00	Mostly Sunny	Dry	19
6	2.6.2025	9:00	Cloudy	Wet	12
7	16.06.2025	11:00	Cloudy	Wet	16
8	14.07.2025	12:30	Mostly Sunny	Dry	28
9	14.07.2025	14:45	Cloudy	Wet	27
10	14.07.2025	15:15	Cloudy	Semi-wet	27

Table 2. Weather conditions of respective passes

This was followed by the dynamic initialization phase, during which the vehicle traverses a calibration section at varying speeds and performs simulated manoeuvres (“weaving”). During the pass through the area of interest, the trajectory is continuously recorded using the integrated GNSS system. After completing the scanning, a dynamic alignment is first performed again, followed by a static alignment.

Figure 5. Data collection pass scheme

5. Data Computing Procedure

After downloading the acquired data from the control unit disks, the point cloud was subsequently processed in the office:

1. Trajectory refinement was performed in POSPac MLS software, where GNSS and IMU data are integrated to achieve maximum positional accuracy. GNSS reference station data were used to support the trajectory refinement.

2. Based on the refined trajectory, individual points of the point cloud were calculated in RiPROCESS software.

3. For the final placement of the point cloud, it was aligned to the control points determined in the previous measurement phase, which serve as the reference framework for transformation into the S-JTSK coordinate system. A non-rigid trajectory method with local adjustment was applied for aligning the point cloud to the control points.

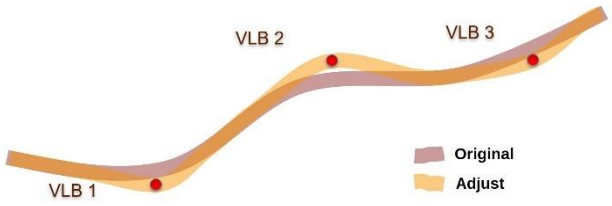

Figure 6. Non-rigid trajectory with local adjustment

The use of a multi-stage procedure (static and dynamic alignment, subsequent trajectory adjustment, and alignment to the control points) minimizes systematic errors and ensures the reliability of the results.
All performed passes were conducted using the identical procedure.

6. Data Processing Procedure

All evaluations were performed using the open-source software CloudCompare, version 2.13.2 [1], which is widely used for the processing and analysis of 3D point clouds. This software enables comprehensive manipulation of point clouds, including cleaning, subsampling, smoothing, and comparison against reference surfaces.

6.1 Data Preprocessing and Clearing

A total of 10 point clouds were available, chronologically labelled 1 through 10. Of these, point clouds 1 - 5 and 8 were acquired under dry conditions, while the remaining 6, 7, 9, and 10 were acquired on wet or partially wet roads.

The first step involved the removal of unwanted objects from the point clouds, particularly stationary or moving vehicles that could distort the results. A combination of automatic software tools (specifically, Tools → Clean → Noise Filter) and manual inspection was used to ensure the removal of all artifacts that could affect subsequent evaluation.

6.2 Subsampling and Data Density Normalisation

The varying vehicle speed during data acquisition, including stops, resulted in an uneven point density. To achieve a homogeneous resolution, the Edit → Subsample function was applied, with a target distance of 3 mm between neighbouring points. Subsampling reduces data redundancy and improves the stability of subsequent deviation calculations.

6.3 Creating Reference Surfaces (Smoothing using MLS)

To determine the dispersion of individual measurements, it was necessary to define the mean (most probable) surface shape. This can be obtained by local smoothing, fitting the point cloud with an appropriate mathematical surface using the least squares method applied to all suitable point clouds together. Smoothing was performed using the function available in CloudCompare via Plugins → PCL wrapper → Smooth using MLS. A second-order polynomial surface was used with a fitting surrounding of 0.04 m, which preserves the local curvature of the surface. Since the measurement system produces higher-quality data when measuring a dry surface, the primary reference point cloud (hereafter DRY cloud) was defined as the average of data acquired under dry conditions. The secondary reference point cloud (WET cloud) was defined analogously from data acquired under wet conditions. Because these reference clouds were generated by merging multiple individual point clouds, their density is unnecessarily high; therefore, after smoothing, these reference datasets were also subsampled to a target distance of 3 mm.

6.4 TIN Reference Surface Transformation

To obtain deviation sign for individual points, a triangular irregular network (TIN, mesh) was created from the reference point clouds. The TIN creation allows the surface composed of points to be approximated using triangles and is suitable for calculating distances from points to the surface. The function Edit → Mesh → Delaunay 2.5D (best fitting plane) was used.

6.5 Calculation of Deviations and Accuracy Characteristics

The deviation values of individual points were determined as distances from the reference TIN surface using the function Tools → Distances → Cloud → Mesh Dist. This step provides a set of deviations that characterize the differences between the measured point cloud and the reference surface.

6.6 Individual Point Clouds Smoothening

Individual point clouds were also smoothed separately because each dataset has a non-zero thickness/depth.

7. Achieved Results

The objective of the analysis was to evaluate the repeatability of MLS results and the influence of weather conditions (dry vs. wet) on the accuracy of mobile laser scanning. Individual point clouds were analysed and compared with reference models created from the benchmark datasets (DRY and WET).
Statistical characteristics were calculated for each of the ten datasets. The results include the achieved values of mean deviation, residual standard deviation, and overall error (RMSE) for each pass. The results of the individual comparisons are presented in tables 3 - 9.

The mean deviation represents the overall average deviation, characterizing possible systematic bias common to the entire point cloud, while the standard deviation represents the residual dispersion around this mean value. In addition, RMSE (Root Mean Square Error) was determined, describing the quadratic mean error characterizing the total error.

$$RMSE = \sqrt{\frac{1}{n}\sum_{i=1}^{n} d_i^2} \qquad (1)$$

where di is the deviation of the respective i-th point from the reference surface and n is the total number of points. RMSE provides a measure of the mean quadratic deviation.
First, a comparison of the DRY and WET benchmark datasets was performed.

mean deviation [m]	standard deviation [m]	RMSE [m]
0,0004	0,0023	0,0023

Table 3. Reference comparison DRY and WET

The results indicate that there practically is no systematic shift between the benchmark datasets.
Next, a comparison of the dry passes against the dry benchmark was performed (using the clean data only).

data	mean deviation [m]	standard deviation [m]	RMSE [m]
1	-0,0002	0,0032	0,0032
2	-0,0005	0,0031	0,0031
3	0,0004	0,0030	0,0030
4	-0,0015	0,0040	0,0043
5	-0,0003	0,0045	0,0045
8	0,0027	0,0036	0,0045
mean	**0,0001**	**0,0036**	**0,0038**

Table 4. Reference DRY – Clean DRY data

The clean point clouds were then smoothed, and the results are presented in the following table.

data	mean deviation [m]	standard deviation [m]	RMSE [m]
1	-0,0002	0,0015	0,0015
2	-0,0005	0,0016	0,0017
3	0,0004	0,0014	0,0015
4	-0,0015	0,0028	0,0032
5	-0,0003	0,0030	0,0030
8	0,0027	0,0021	0,0034
mean	**0,0001**	**0,0022**	**0,0025**

Table 5. Reference DRY – Smooth DRY data

The same analyses were then performed for the individual wet passes, compared against the DRY reference.

data	mean deviation [m]	standard deviation [m]	RMSE [m]
6	-0,0002	0,0049	0,0049
7	0,0007	0,0040	0,0041
9	0,0016	0,0047	0,0050
10	-0,0008	0,0052	0,0053
mean	**0,0003**	**0,0047**	**0,0048**

Table 6. Reference DRY – Clean WET data

data	mean deviation [m]	standard deviation [m]	RMSE [m]
6	-0,0002	0,0034	0,0034
7	0,0007	0,0020	0,0021
9	0,0016	0,0030	0,0034
10	-0,0008	0,0043	0,0044
mean	**0,0003**	**0,0033**	**0,0034**

Table 7. Reference DRY – Smooth WET data

The results indicate that the wet passes show approximately 1 mm worse performance relative to the dry benchmark.
Next, a comparison of the wet passes against the WET benchmark was performed.

data	mean deviation [m]	standard deviation [m]	RMSE [m]
6	-0,0006	0,0041	0,0041
7	0,0002	0,0038	0,0038
9	0,0012	0,0058	0,0059
10	0,0011	0,0040	0,0041
mean	**0,0005**	**0,0045**	**0,0046**

Table 8. Reference WET – Clean WET data

data	mean deviation [m]	standard deviation [m]	RMSE [m]
6	-0,0006	0,0019	0,0020
7	0,0002	0,0016	0,0016
9	0,0011	0,0023	0,0025
10	0,0011	0,0027	0,0029
mean	**0,0005**	**0,0022**	**0,0023**

Table 9. Reference WET – Smooth WET data

The results indicate the following:
Comparison of the reference datasets DRY x WET: the overall elevation shows practically no systematic difference - 0.4 mm. The overall data dispersion on the wet surface is higher - dry RMSE: 3.8 mm (clean) and 2.5 mm (smooth); wet RMSE: 4.8 mm (clean) and 3.4 mm (smooth). Analysis of the wet passes shows that problematic areas occur in locations where a thicker layer of water was present during the pass, resulting in very high surface dispersion (e.g. 20 cm). In some cases, the underlying surface is captured beneath this noise. In other cases it is not, and after noise removal, holes appear in the point cloud. This phenomenon can be observed at figure 7 left (noise) and right (holes).
In the hypsometric model shown on figure 8, the problematic areas with higher water occurrence are visible. This corresponds to the DRY benchmark versus wet pass no. 9.

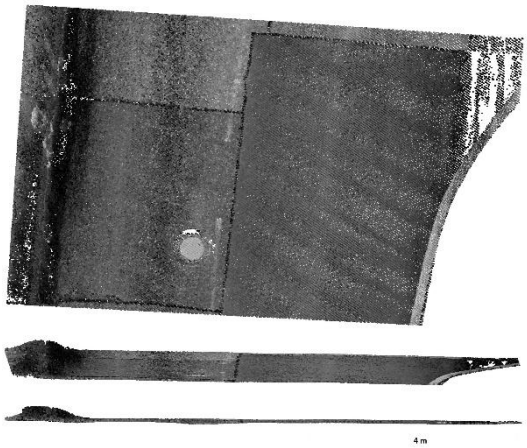

Figure 7. Local cloud disturbances (wet pass no. 9)

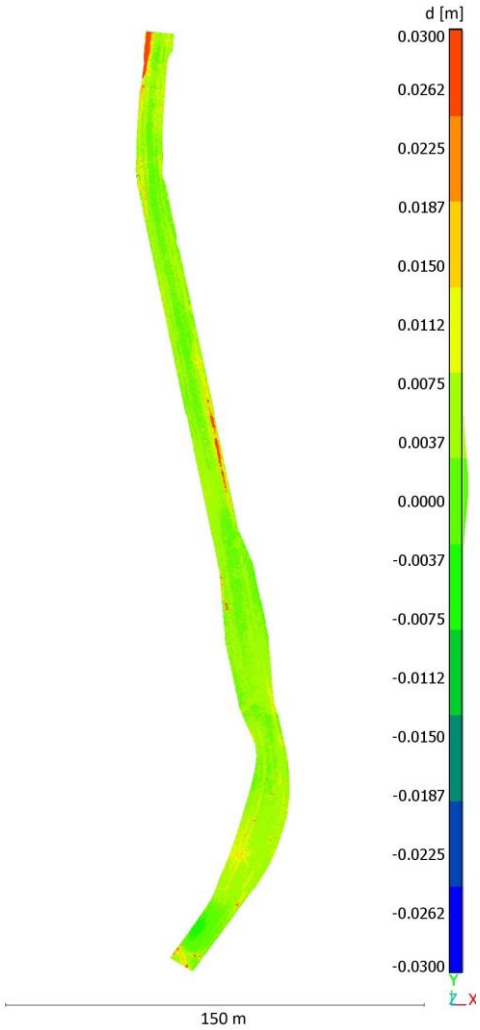

Figure 8. Hypsometric representation of deviations (wet pass no. 9)

In the figure 9 is detail showing the ruts in the asphalt of the road from heavy traffic where the water level is higher (in red).

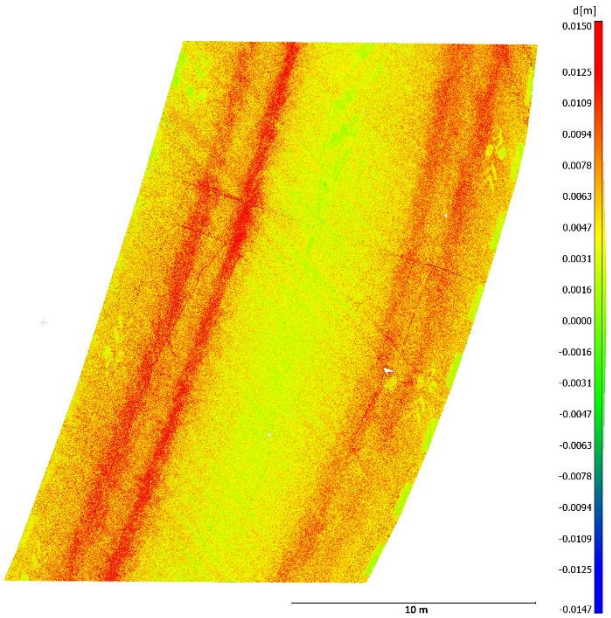

Figure 9. Hypsometric representation of deviations (wet pass no. 9) – detail

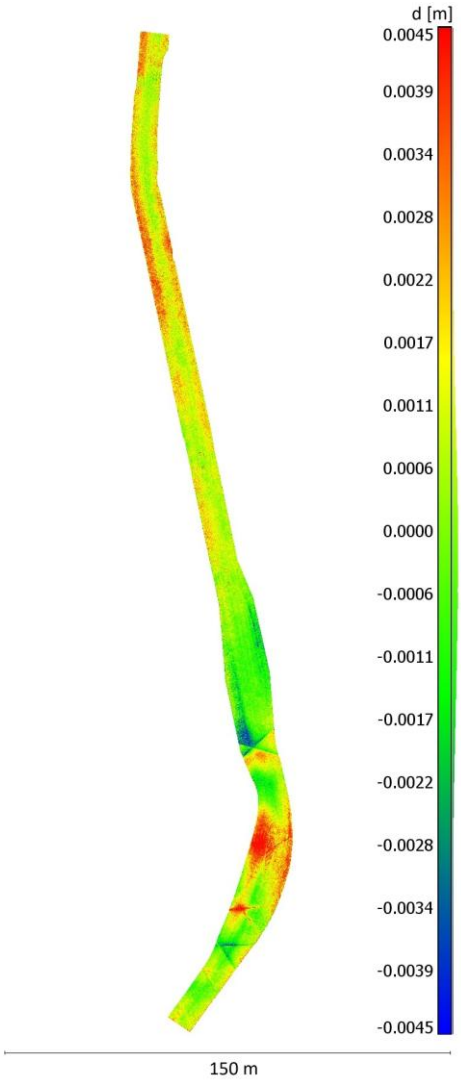

Figure 10. Hypsometric representation of deviations (dry pass 1)

For comparison, one can look at figure 10, where dry pass 1 deviations is also shown hypsometrically. It is worth noting the scale range, which is only ± 4.5 mm here.

8. Conclusion

The achieved results indicate that by following an identical data acquisition and processing procedure, it is possible to achieve results with a standard deviation better than 3 mm and practically no systematic influence. Furthermore, the effect of a wet surface is also evident; in addition to increased value dispersion, pronounced local disturbances also occur. From the RMS and standard deviation results, compliance with the accuracy specified by the manufacturer is apparent.

Acknowledgements

At this point, we would like to thank to prof. Ing. Martin Štroner, Ph.D. for his help and advice evaluating and processing the acquired data in CloudCompare software.

References

CloudCompare Development Team, 2021. CloudCompare User Manual Version 2.6.1. https://www.cloudcompare.org/doc/qCC/CloudCompare%20v2.6.1%20%20User%20manual.pdf (12 July 2025).

Štroner, M. 2013: Laserové skenování v inženýrské geodézii. ČVUT in Prague, Faculty of Civil Engineering.

RIEGL Laser Measurement Systems GmbH. 2019. RIEGL VMX-2HA: High Speed, High Performance Dual Scanner Mobile Mapping System. http://www.riegl.com/uploads/txpxpriegldownloads/RIEGL_VMX-2HA_brochure_2024-09-30.pdf (12 July 2025).

Hampacher, M., Štroner, M. 2015: Zpracování a analýza měření v inženýrské geodézii. 2nd ed. Praha: Česká technika - nakladatelství ČVUT, ČVUT in Prague, 336 s. ISBN 978-80-01-05843-5.